

# Membrane distillation of power plant cooling tower blowdown water

Elif İnce\* and Yasin Abdullah Uslu

Gebze Technical University, Department of Environmental Engineering, Kocaeli, Turkey

(Received October 6, 2018, Revised March 15, 2019, Accepted April 9, 2019)

**Abstract.** The objective of this study was to examine the recovery of the power plant cooling tower blowdown water (CTBD) by membrane distillation. The experiments were carried out using a flat plate poly vinylidene fluoride (PVDF) membrane with a pore diameter of 0.22  $\mu\text{m}$  by a direct contact membrane distillation unit (DCMD). The effects of operating parameters such as transmembrane temperature difference ( $\Delta T$ ), circulation rate and operating time on permeate flux and membrane fouling have been investigated. The results indicated that permeate flux increased with increasing  $\Delta T$  and circulation rate. Whereas maximum permeate flux was determined as 47.4  $\text{L}/\text{m}^2\cdot\text{h}$  at  $\Delta T$  of 50°C for all short term experiments, minimum permeate flux was determined as 7.7  $\text{L}/\text{m}^2\cdot\text{h}$  at  $\Delta T$  of 20°C. While 40°C was determined as the optimum  $\Delta T$  in long term experiments. Inorganic and non-volatile substances caused fouling in the membranes.

**Keywords:** power plant; cooling tower blowdown water; membrane distillation; flux; circulation rate; transmembrane temperature difference

## 1. Introduction

Water plays a critical role in modern thermo-electrical energy industry. It works as the physical source of energy transformation and the medium for heat exchange. Two important water cycles are used in a typical thermal power plant with cooling tower. In the first cycle high quality boiler water is converted into steam by way of a closed cycle and activates a steam turbine that provides power to an electric generator. Another recirculation water circuit removes the heat from the condenser at the low pressure side of the steam turbine and distributes the heat inside this cooling tower by way of evaporation. Large amounts of water are consumed to support power generation. Cooling tower blowdown water (CTBD) is typically drawn from the fresh water source. Contaminants in the cooling water circuit such as  $\text{Ca}^{2+}$ ,  $\text{Mg}^{2+}$ ,  $\text{CO}_3^{2-}$  and  $\text{HCO}_3^-$ , silica, microorganisms and chemicals increase due to the evaporation, leakage, and wind effect, leading to scale formation and corrosion. Concentrated water is discharged and fresh water is added to the tower in order to prevent scale formation and corrosion. For example, a 300 MW electricity producing power plant recirculates about 20,000  $\text{m}^3/\text{hour}$  cooling water and generates about 98  $\text{m}^3/\text{hour}$  of blowdown (Zhang *et al.* 2007). In general, about 10-20% of the consumed water results in blowdown and the remainder evaporates (Yu *et al.* 2013).

Limited amount of freshwater, environmental protection and cost reduction act as driving forces for treating CTBD and its reuse. Just like softening with lime-soda (Mattson and Harris 1979), chemical coagulation and brine thermal

evaporation (Di Filippo 2004) are typical treatment approaches for CTBD. Lime-soda softening eliminates hardness; however it also consumes up the chemicals and requires the disposal of the sludge that forms as a result of softening. Thermal evaporation with mechanical steam recompression may generate large amounts of distillate and provides high water recovery while consuming large amounts of electricity ( $\sim 20\text{-}25 \text{ kWh}/\text{m}^3$ ). Membrane technologies as alternative treatment methods have attracted significant attention in recent years. Microfiltration (MF), ultrafiltration (UF) and nanofiltration (NF) have been used as pre-treatment for the removal of particles, bacteria, colloids and silica (Zhang *et al.* 2007). For industrial applications, membrane capital cost and fouling problems are two significant challenge to be resolved. RO is considered as the most reliable and cost effective membrane salt removal technology as of now. It consumes less energy in comparison with thermal distillation systems and generates relatively higher quality water. But, chemicals in CTBD along with waste chlorine, silica and minerals which can cause fouling have adverse impacts on RO performance. Residual chlorine and chlorine oxide may damage the RO membrane (Shintani *et al.* 2009). RO membranes have low resistance against colloidal or reactive silica. Finally, RO is not convenient for high concentration water due to high osmotic pressure and it has been also observed that it is not always sufficient for the rejection of all dissolved species (Greenlee *et al.* 2009, Plakas and Karabelas 2012).

The aforementioned disadvantages of RO can be overcome by membrane distillation (MD) which is emerging salt removal technology. MD is a combined system comprised of thermal distillation and membrane processes. Basic separation mechanism is the vapor-liquid balance theory (El-Bourawi *et al.* 2006, Gryta 2012, Kim *et al.* 2017). The driving force for mass transfer in MD is the vapor pressure difference across the membrane due to

\*Corresponding author, Associate Professor  
E-mail: e.senturk@gtu.edu.tr

temperature difference. The hot feed side should be in contact with the membrane; however the vapor that passes through the micro-pores may be carried by different media such as water, vacuum, air and gas. According to these media, the MD process is named as direct contact MD (DCMD), vacuum MD (VMD), air gap MD (AGMD) and sweeping gas MD (SGMD), respectively (Loussif and Orfi 2016). When MD process is compared with other desalination processes such as RO and thermal distillation, the advantages of MD can be listed as follows: (i) lower operating temperature vapor area in comparison with conventional distillation; (ii) lower operating pressure and membrane fouling in comparison with RO; (iii) rejection of salt and non-volatile components up to 100%; (iv) unlimited in view of high osmotic pressure; and (v) much lower energy costs when waste or low degree heat is used (Yu *et al.* 2013). In MD, the membrane material should be hydrophobic and chemically inert. Hence materials such as polyvinylidene difluoride (PVDF), polytetrafluoroethylene (PTFE) and polypropylene (PP) are often used for MD membrane (Boubakri *et al.* 2014).

DCMD is the most used MD process for laboratory studies (Meng *et al.* 2015, Zougrana *et al.* 2016). In this system, the hydrophobic membrane is in direct contact with the liquid phases. Feed water is located on one side of the membrane and distilled water on the other. The process is mainly affected from vapor pressure and temperature changes and less from concentration polarization and changes in pH (El-Bourawi *et al.* 2006, Gryta 2009). DCMD is considered to be the best application and the simplest design for the desalination of various types of salty waters such as sea water (Shirazi *et al.* 2012), brackish water (Hou *et al.* 2010), brine (Ji *et al.* 2010) and synthetic salt water (Martinez-Diez and Vazquez-Gonzalez 1999).

In literature, CTBD and MD is quite low despite the fact that there are many different MD studies with different water/wastewater. Thus, in this study, the impacts of various operating parameters such as transmembrane temperature difference ( $\Delta T$ ), circulation rate and operation time on the recovery of CTBD by DCMD method and on membrane fouling have been investigated.

## 2. Experimental design

### 2.1 Wastewater and analytical methods

The CTBD used in this study was obtained from the cooling tower of a 51 MW power plant. About 104 m<sup>3</sup> water per hour has been used in the process as cooling water. Chemicals such as 96% H<sub>2</sub>SO<sub>4</sub> for pH control, corrosion inhibitor (Green wet treat 90007), hardness inhibitor (Green wet treat 1297) and sulfate inhibitor (Green wet treat 1058-P) have been added to the cooling water. The cooling water used has been directly discharged to the river (7 m<sup>3</sup>/hour). CTBD was placed in 25 L drums from the cooling tower and it was brought into the laboratory and stored at +4°C. Conductivity and pH parameters were measured on site and the other parameters were analyzed in the laboratory. The characterization of the waste water obtained from the plant have been presented in Table 1.

Table 1 Characterization of CTBD obtained from the thermal plant

Parameter	Unit	Value
TCOD	mg/L	33.8
DCOD	mg/L	25.6
TOC	mg/L	10.12
Conductivity	mS/cm	5.52
pH	-	8.05
Sulfate	mg/L	4508.10
Chlorine	mg/L	104.30
Hardness	mg CaCO <sub>3</sub> /L	4300.00
Nitrate	mg/L	6.40
Phosphate	mg/L	5.52
Silica	mg/L	35.83
Calcium	mg/L	355.30
Magnesium	mg/L	550.00
Sodium	mg/L	1.84
Potassium	mg/L	19.71
Iron	mg/L	0.04
Manganese	mg/L	0.23
TKN	mg/L	3.90
TSS	mg/L	6.40
TDS	mg/L	6537.20

The distillate acquired at the end of every experiment was also analyzed. Conductivity and pH measurements were made with conductivity/pH meter (WTW multiline P4). Total Suspended Solids (TSS), Total Dissolved Solids (TDS), Total Kjeldahl Nitrogen (TKN), hardness, Total Chemical Oxygen Demand (TCOD), and Dissolved COD (DCOD) were analyzed according to APHA (2005). In addition, TOC measurement device (TOC-L, Shimadzu) was used on the samples for determining the TOC concentration via NPOC (non-purgeable organic carbon) method. Sulfate and chlorine concentrations were determined using IC device (Shimadzu). The analyses were carried out in the IC-SA2 column with 1 mL/min. flow rate at 70 bar and the duration of analysis was 15 minutes. Ca, Mg, K, Fe and Si were determined with ICP-OES (Perkin Elmer). Nitrate determination was carried out using a ready kit (Hach Lange LCK-339). Furthermore, phosphate analysis was carried out in accordance with STM 4500-P-D (APHA 2005).

### 2.2 Membrane and Membrane module

A flat sheet, hydrophobic and micro-porous PVDF (Millipore) membrane was used for membrane distillation of CTBD. The fundamental properties of the membrane used have been given in Table 2. It is a symmetrical membrane without support layer on any side.

Table 2 Fundamental properties of the membrane used in the study

Material	PVDF hydrophobic
Average pore dimension ( $\mu\text{m}$ )	0.20
Thickness ( $\mu\text{m}$ )	$\approx 200$
Porosity (%)	75
Contact angle ( $^\circ$ )	$130 \pm 1$

A Teflon module was made in order to fix the PVDF membrane and to ease the flow channels. The module is comprised of two symmetrical flat Teflon plates. The thickness of each Teflon plate is 2 cm in order to reduce heat loss from the module to the environment. A small flow conduit was engraved on one side of each plate and a support/spacer with a thickness of 0.5 mm and gap of 2.5 mm was placed. The length, width and height of the small conduit were 4.5 cm, 0.5 cm and 1.25 cm respectively. The effective contact area of water was  $59.3 \text{ cm}^2$  due to the overlapping of the hermetic seal and membrane. Following the installation, the module was dried during 5 minutes using 12-14 psig pressurized air to ensure the hydrophobicity of the membrane.

### 2.3 DCMD installation and test procedure

The studies were carried out using a laboratory scale DCMD setup. The schematic diagram of the experimental setup has been presented in Fig. 1. The system has a Teflon membrane module in contact with two thermostatic cycles (feed and permeate). The hydrophobic membrane is between these two compartments. Feed and permeate temperatures were measured for each compartment using a digital thermometer with a sensitivity of  $\pm 0.1^\circ\text{C}$ . In addition, feed and distillate flows were carried out in a cross flow configuration. CTBD kept at constant temperature via a water bath (Daihan Scientific Maxircu CL) was given to the membrane distillation module by way of a peristaltic pump (Omega FPU5-MT). The distillate that heats up with the condensed permeate was cooled using a cooler (Julabo F12) and passed through the module by way of another peristaltic pump (Omega FPU5-MT). K type thermocouple sensors and high resolution pressure indicators (0-6 psig) were adjusted for monitoring the inlet and outlet temperature and pressure values. Conductivity and pH sensors were also placed in the feed and distillate tanks. A precision balance (AND EJ-6100) was used for determining membrane flux at each operating condition.

A study procedure was followed for evaluating DCMD after installation. Deionized water ( $0.8\text{-}1.0 \mu\text{S}/\text{cm}$ ) was used for rinsing until the cold water conductivity for both hot and cold cycles reached the  $1.0\text{-}3.0 \mu\text{S}/\text{cm}$  interval. During the experiments, 17 L CTBD was placed in the feed tank for long term experiments and 2 L for short term experiments and about 500 mL deionized water was left in the distillate tank for ensuring the circulation of the cold side. The tanks at both sides were covered for preventing loss of vapor. The water at the feed side was heated up to the desired

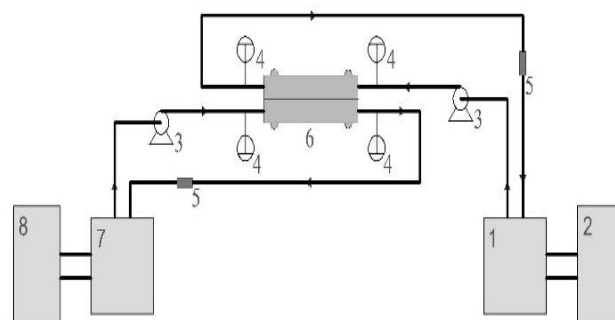


Fig. 1 MD Experiment Setup (1-Permeate Tank, 2-Cooling System, 3-Peristaltic Pump, 4-Thermocouples, 5-Conductivity and pH Measurement Probe, 6- Layer Membrane Module, 7-Feed Tank, 8-Water Circulator)

Table 3 Characterization of CTBD obtained from the thermal plant

Parameter	Unit	Value
Feed temperature (FT)		40
		50
		60
		70
Permeate temperature (PT)	$^\circ\text{C}$	20
		20
Transmembrane temperature difference ( $\Delta T = FT - PT$ )		30
		40
		50
Feed cross flow rate		0.169
	m/s	0.337
		0.730

temperature using a water bath by way of a bypass circuit. The distillate cross flow rate was kept constant during all experiments ( $0.337 \text{ m/s}$ ) and the system was tested at different transmembrane temperature differences and flow rates of feed (Table 3). The system was operated for about 6 hours during each short term experiment. A long term (about 50 hours and 75 hours) DCMD study was carried out for the two different temperature differences and the same flow rate determined at the end of these experiments.

### 2.4 Fouling characterization and evaluation of system performance

Morphological images of the clean and used membrane were acquired by scanning electron microscopy (SEM). Energy distribution spectrometer (EDS) enabled the determination of the inorganic elements on the surface of the foul membrane. The Fourier transformation infrared (FTIR) spectrum of the samples was measured using a scattered infrared spectrophotometer (IR Prestige-21, SHIMADZU).

Conductivity and pH values for CTBD and distillate water were recorded to the computer by a monitor (WTW Multiline P4) throughout the experiment.

DCMD specific flux,  $J$  was calculated using the formula

given below:

$$J = \frac{(W_2 - W_1)}{A \times t} \quad (1)$$

Here,  $(W_2 - W_1)$  (kg) represents the increase in weight during recording.  $A$  ( $m^2$ ) denotes the membrane area and  $t$  (hours) is duration of the distillate water collection.

Non-volatile dissolved substances were kept in the CTBD throughout the DCMD process. Rejection efficiency ( $R$ , %) was calculated using the equation given below;

$$R (\%) = \frac{(\text{Feed conductivity} - \text{Permeate Conductivity})}{\text{Feed conductivity}} \times 100 \quad (2)$$

### 3. Results and discussion

#### 3.1 Permeate flux and conductivity throughout the operation

Many parameters such as temperature, feed pH, feed concentration, crossflow rate, and membrane properties, operating time and fouling have various impacts on flux (Manna *et al.* 2010, Zoungrana *et al.* 2016). MD is the non-isotherm membrane separation process and the transmembrane temperature difference ( $\Delta T$ ) between the feed and cold sides is accepted as the dominant operating parameter that affects permeate flux. The impact of  $\Delta T$  on DCMD permeate flux has been examined in range of 20 – 50°C at a constant permeate temperature of 20°C. The  $\Delta T$  between membrane feed and permeate surfaces increases the driving force at high feed temperature. Larger amount of steam is generated from a feed solution that causes a higher vapor pressure thereby resulting in an increase of flux from the membrane pores.

Every DCMD experiment was carried out till reaching the steady flux. The behavior of permeate flux as a function of operating time has been presented in Fig. 2 and Fig. 3.

As can be seen from Fig. 2, permeate flux slightly decreased in all experiments and average flux values were 7.7 L/m<sup>2</sup>·h, 14.8 L/m<sup>2</sup>·h, 28.8 L/m<sup>2</sup>·h and 47.4 L/m<sup>2</sup>·h for 20°C, 30°C, 40°C, and 50°C, respectively. Whereas the maximum permeate flux was measured at  $\Delta T$  of 50°C, minimum permeate flux was determined at  $\Delta T$  of 20°C. In addition, it can be understood from Fig. 2 that flux increases with increasing temperature difference (Zoungrana *et al.* 2016, Boubakri *et al.* 2017, Kim *et al.* 2017). Kujawa and Kujawski (2015) reported that the driving force of the DCMD system ( $\Delta P$ ) depends to a great extent on the temperature difference between feed and permeate ( $\Delta T$ ) rather than the temperature of the feed solution alone. Furthermore, they have also put forth that the driving force increases at constant  $\Delta T$  value depending on the increase in feed temperature. In this study, cooling permeate temperature was observed and kept constant at 20°C, any increase in feed temperature resulted in an increase in  $\Delta T$  and thereby a higher  $\Delta P$  according to the Antoine equality (Ge *et al.* 2014). No decrease over time was observed in flux during these short term (6 hours) experiments. Therefore, it is observed that no significant decrease in the permeate flux is observed in the DCMD application

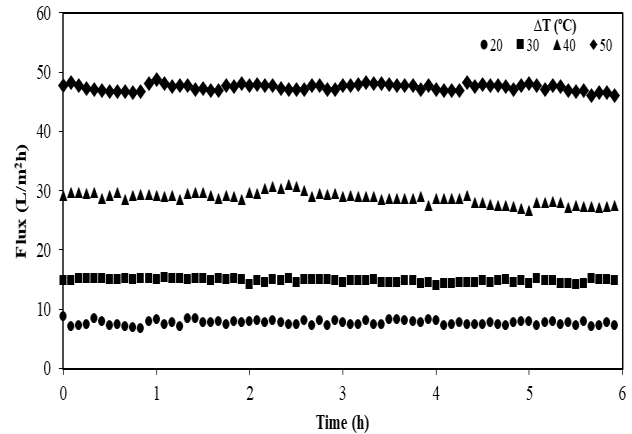


Fig. 2 Flux obtained for different  $\Delta T$  ( $v = 0.73$  m/s)

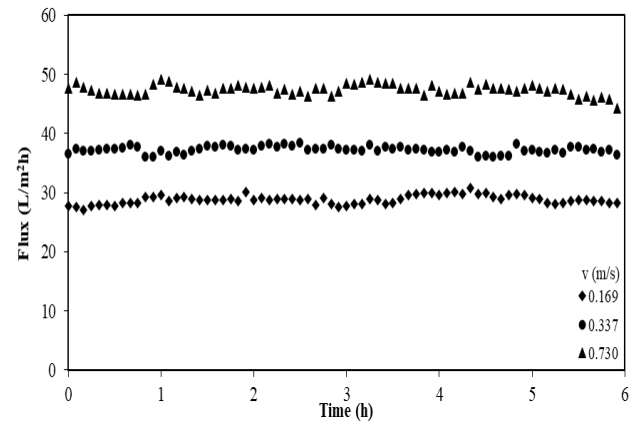


Fig. 3 Flux obtained for different feed circulation rates (at  $\Delta T = 50^\circ\text{C}$ )

(Zoungrana *et al.* 2016, Boubakri *et al.* 2017) and that it is advantageous for the removal of salt from CTBD.

With regard to water quality, conductivity of permeate increased slightly from 1.0 to 6.0  $\mu\text{S}/\text{cm}$  in short term studies and remained constant over time. A slight increase in permeate conductivity indicates that DCMD has displayed a highly stable performance and that wastewater has not caused issues related with membrane wettability or fouling phenomena. Similar results have been observed in DCMD studies in the literature (Boubakri *et al.* 2017).

The flux values acquired at  $\Delta T$  of 50°C during short term experiments with different circulation rates have been presented in Fig. 3. As can be seen in the Fig. 3, the flux passing through the membrane increased with increasing circulation rate since temperature polarization decreased due to the increase in flow turbulence. The average flux values were 28.8 L/m<sup>2</sup>·h, 37.2 L/m<sup>2</sup>·h, and 47.4 L/m<sup>2</sup>·h for 0.169 m/s, 0.337 m/s, and 0.730 m/s, respectively. No significant decrease in flux was observed during these short term experiments.

Increase in flow rate increased the Reynolds number representing the flow type which decreased the thickness of the membrane border layer, resulting in heat transfer coefficient increased (Ge *et al.* 2014). Thus, the surface

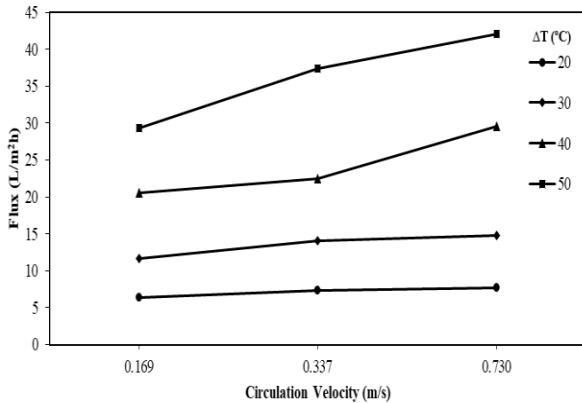


Fig. 4 Average flux values obtained for different circulation rates at different  $\Delta T$

temperature of the membrane increased to a value close to that of the feed temperature thereby increasing the mass transfer force at both sides of the membrane. This indicates that increasing flow rate decreases both heat polarization and concentration polarization.

Reynolds number ( $Re$ ), expressed by Eq. 3, can be used to characterize fluid flow state.

$$Re = \frac{\rho \vartheta D}{\mu} \quad (3)$$

Here,  $\rho$  denotes density ( $\text{kg/m}^3$ ),  $\vartheta$  is velocity ( $\text{m/s}$ );  $D$  is hydraulic diameter ( $\text{m}$ ), and  $\mu$  is the viscosity of the fluid ( $\text{kg/ms}$ ). Fluid flow is in the laminar flow regime when  $Re < 2000$  and in turbulent flow regime when  $Re > 4000$ .

The character of the flow state is one of the effective parameters on permeate flux (Shirazi and Kargari 2015). In this study, CTBD circulation flow was adjusted to where could not be a turbulent flow ( $Re < 4000$ ) in the experiments. The  $Re$  values calculated at  $\Delta T$  of  $50^\circ\text{C}$  were 911.8, 1605.0, and 3476.7 for flow rate of 0.169 m/s, 0.337 m/s, and 0.73 m/s, respectively.

The impact of hydrodynamic conditions on permeate flux can be clearly seen in Fig. 4. The permeate flux increases with increasing circulation rate resulting in increasing Reynolds number. The impact of temperature and concentration polarization decreases with increasing Reynolds number, resulting in decrease in heat and mass transfer resistances (Pal and Manna 2010, He *et al.* 2011). This is an indication that the membrane surface temperature is close to the feed CTBD temperature, providing in a greater transmembrane temperature difference. Therefore, the increase in driving force results in an increase in flux. As can be seen from Eq. 3,  $Re$  number increases with increasing CTBD temperature due to decrease in viscosity. Therefore, it is expected that permeate flux increase with both increasing circulation rate and  $\Delta T$ . Boubakri *et al.* (2017) reported that permeate flux increases at a significant level with increasing Reynolds number at  $Re < 4000$ , whereas it increases slightly with increasing Reynolds number at  $Re > 4000$ .

Decrease in flux over time along with deterioration in distillate quality may occur in MD applications with increasing  $\Delta T$ , which leads to membrane fouling and

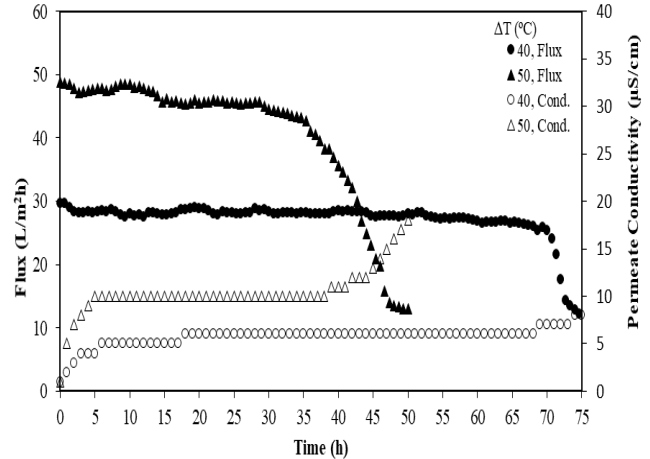


Fig. 5 Long term operational flux graph for  $\Delta T = 40^\circ\text{C}$  and  $\Delta T = 50^\circ\text{C}$

wetting due to an increase in flux. Therefore, long terms studies were carried out at cross flow rate of 0.73 m/s for  $\Delta T$  of 40 and  $50^\circ\text{C}$  since highest permeate flux were obtained at these operation conditions during short term DCMD. The flux values obtained as a result of these studies have been given in Fig. 5.

As can be seen in Fig. 5, permeate flux remained almost constant at  $\Delta T$  of  $40^\circ\text{C}$  during 70 hours. The permeate flux being  $28.1 \text{ L/m}^2\cdot\text{h}$  at the end of 70 hours decreased rapidly down to  $13 \text{ L/m}^2\cdot\text{h}$ . No significant increase in distillate conductivity was observed during this decrease, which indicates that flux decrease may be due to membrane fouling. Whereas permeate flux remained constant for 35 hours at  $\Delta T$  of  $50^\circ\text{C}$ , it decreased rapidly at the end of 35 hours. The conductivity of the obtained distillate was relatively higher in comparison with that of distillate at  $\Delta T$  of  $40^\circ\text{C}$ . At  $\Delta T$  of  $50^\circ\text{C}$ , both the decrease in flux and the increase in distillate conductivity may be due to various reasons; (i) a sudden increase in flux and an increase in distillate conductivity is observed when membrane is wetted taking place relatively more easily at higher temperatures (Ge *et al.* 2014). (ii) Concentration polarization of salt ( $\text{CaSO}_4$ ) crystals at the interface, resulting in a decrease in both the diffusion coefficient of the water molecules and the diffusion ratio at the hot side. F-TIR, SEM and EDS analyzes have been used for carrying out detailed investigation of membrane fouling in the system operated at both temperature differences.

Membrane wetting is more observed at higher temperatures since the salt in the feed accelerates the membrane wetting due to decrease in its solubility (Ge *et al.* 2014). Furthermore, the decrease in membrane hydrophobicity of the fouled membrane results in membrane wetting. Membrane wetting causes a decrease in flux and an increase in distillate conductivity. Fig. 5 shows that the electrical conductivity of the distillate is higher at  $\Delta T$  of  $50^\circ\text{C}$  in comparison with  $\Delta T$  of  $40^\circ\text{C}$ . The change in the conductivity of the distillate indicated that the membrane was wetted and that wetting was more significant at higher temperatures.

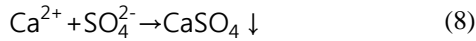
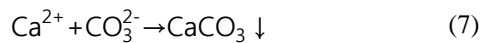
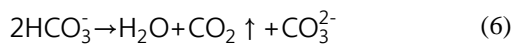
It is reported, in the literature that there are two reasons of membrane wetting. The first is that increase in feed

temperatures regardless of CTBD characterization causes a decrease in the surface tension at the feed and thus a decrease in fluid inlet pressure (Ge *et al.* 2014) thereby making the membrane wet more easily. The other reason is that the enlargement of membrane pores with temperature is effective in membrane wetting (Saffarini *et al.* 2013).

On the other hand, temperature polarization increased with increasing temperature and the viscosity of the CTBD decreased which was convenient for the increasing of permeate flux. This result was in accordance with those of other studies which utilized DCMD (Peng *et al.* 2005).

### 3.2 Membrane Fouling and Its Morphology

Membrane scaling causes decrease in both flux and salt rejection (Gryta 2010). CTBD has high silica content and high hardness. Contaminant and ion concentration of the feed increase depending on the acquired flux from the beginning of the DCMD process. It was possible that the following equilibrium reactions took place related with the concentration process in this study (Yu *et al.* 2013).



Scale formation rate on the membrane surface is determined by various factors such as supersaturation level, water temperature, flow conditions, membrane surface roughness and characterization of the feed water (CTBD) (Koyuncu and Wiesner 2007, Gryta, 2009). Contrary to homogeneous nucleation taking place in the feed water, crystal nucleation on the membrane surface is occurred as heterogeneous nucleation (Gryta 2009).

Co-precipitation tendency of  $\text{CaSO}_4$  and  $\text{CaCO}_3$  is affected from the both feed water composition and hydrodynamic conditions, playing a role on concentration polarization (Koyuncu and Wiesner 2007). Feed flow rate has a significant impact on the morphology of the  $\text{CaCO}_3$  sediment. Likewise, larger crystals are formed at lower feed flow rates and the generated  $\text{CaCO}_3$  layer is more compact than those that develop in faster flow rates (Gryta 2009).

The membrane surface can be covered with contaminants in MD, which reduces effective pore region and the temperature gradient between the feed and permeate sides and finally the permeate flux (Kim *et al.* 2017). The SEM morphology of the membrane at the hot CTBD side surface can be seen in Fig. 6. It can be seen from the SEM images that there is no significant fouling and/or scaling on the membrane in short term DCMD applications. However, it is thought that scaling on the membrane increases depending on the decrease of the solubility of ions such as silica, Ca and Mg with increasing  $\Delta T$ . It was observed that the CTBD characterization had no significant impact for short term DCMD applications. However, it can be seen in

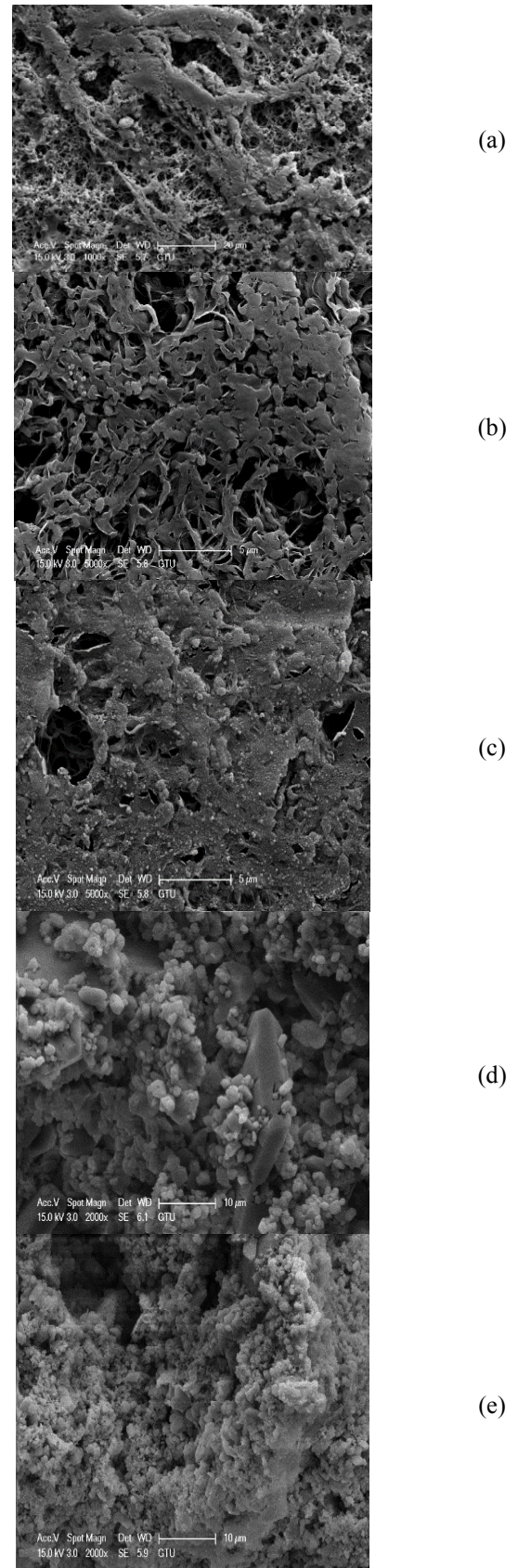


Fig. 6 SEM images of clean membrane and the membranes used in the study (a: Clean membrane, b:  $\Delta T=20^\circ\text{C}$ ,  $v=0.337$  m/s and  $t=6$  hours, c:  $\Delta T=50^\circ\text{C}$ ,  $v=0.337$  m/s and  $t=6$  hours, d:  $\Delta T=40^\circ\text{C}$ ,  $v=0.73$  m/s and  $t=75$  hours, e:  $\Delta T=50^\circ\text{C}$ ,  $v=0.73$  m/s and  $t=50$  hours)

Figs 6d and 6e that a significant amount of fouling and scaling developed on the membrane in long term DCMD applications. This indicates that CTBD characterization gains importance in long term operations. It can be observed, compared with  $\Delta T$  of  $40^{\circ}\text{C}$ , that flux decreased and that distillate conductivity increased and that fouling/scaling on the membrane surface for  $\Delta T$  of  $50^{\circ}\text{C}$  was higher.

EDS analysis of the fouling membrane was carried out (Fig. 7). It was determined that clean membrane only had C (48.1%) and F (51.9%). Similar results were reported by Kim *et al.* 2017. No distinctive difference was observed in membranes taken from short term DCMD system. Measurements for  $\Delta T$  of  $20^{\circ}\text{C}$ ,  $v = 0.337$  m/s and  $t = 6$  hours were C (49.21%), O (0.10%) and F (50.69%) while measurements for  $\Delta T$  of  $50^{\circ}\text{C}$ ,  $v = 0.337$  m/s and  $t = 6$  hours were C (49.02%), O (0.35%) and F (50.63%). As expected, it was determined that many inorganic substances accumulated on the membrane surface as a result of measurements on membranes from long term experiments. The inorganic elements determined for  $\Delta T$  of  $40^{\circ}\text{C}$  and circulation rate of 0.73 m/s were C (3.93%), O (51.44%), Mg (0.24%), Si (0.75%), S (22.82) and Ca (20.82%). However, the inorganic elements determined for  $\Delta T$  of  $50^{\circ}\text{C}$  and circulation rate of 0.73 m/s were C (5.07%), O (33.41%), Mg (3.27%), Si (11.59%), S (21.73) and Ca (24.94%). Elementary analysis indicates scaling on the membrane. It can be concluded that fouling on the membrane was lower at  $\Delta T$  of  $40^{\circ}\text{C}$  based on both the SEM images and the EDS analysis results as well as the flux graphs obtained. It is also noteworthy that fouling was observed on the membranes in long term applications whereas no significant difference was observed between the membranes used in short term applications and clean membranes.

F-TIR analysis was also conducted on the clean and used membranes. The spectra acquired as a result of the analyses have been given in Fig. 8. A peak was observed at the  $1000\text{--}1400\text{ cm}^{-1}$  band for C-F, as expected, from the clean membrane (Liu *et al.* 2010). In addition, the peak observed at  $3025\text{ cm}^{-1}$  is an indication of the C-F band vibration (Liu *et al.* 2010). The same peaks were observed at the aforementioned bands in all the membranes used in this study. It can be clearly seen in FTIR spectra from Fig. 8 that no gypsum ( $\text{CaSO}_4 \cdot 2\text{H}_2\text{O}$ ) was formed in short term applications but there was gypsum formation in long term applications ( $670\text{ cm}^{-1}$ ,  $1614\text{ cm}^{-1}$ ) (Yu *et al.* 2013).

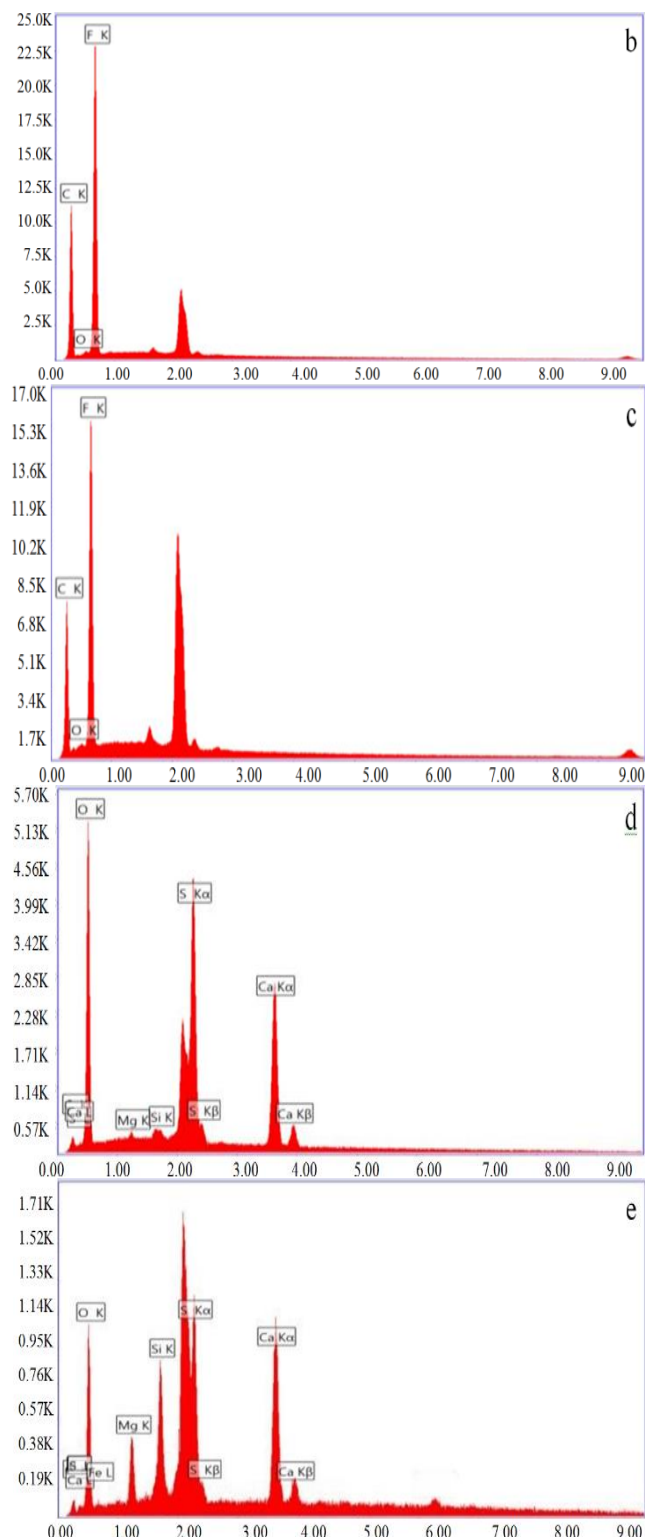
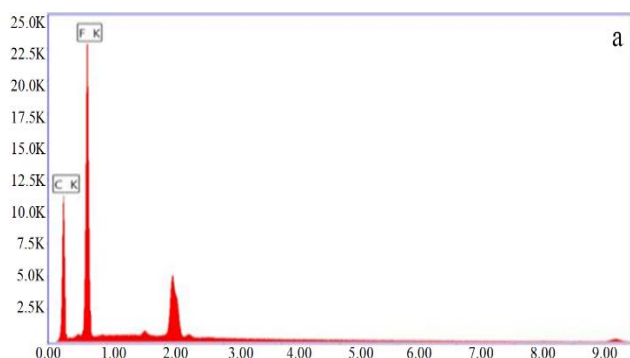


Fig. 7 EDS images of clean membrane and the membranes used in the study (a: Clean membrane, b:  $\Delta T=20^{\circ}\text{C}$ ,  $v=0.337$  m/s and  $t=6$  hours, c:  $\Delta T=50^{\circ}\text{C}$ ,  $v=0.337$  m/s and  $t=6$  hours, d:  $\Delta T=40^{\circ}\text{C}$ ,  $v=0.73$  m/s and  $t=75$  hours, e:  $\Delta T=50^{\circ}\text{C}$ ,  $v=0.73$  m/s and  $t=50$  hours)

In addition, calcite peaks ( $1453\text{ cm}^{-1}$  and  $873\text{ cm}^{-1}$ ) were observed in the analysis of the long term application membranes (Yu *et al.* 2013). It is thought that silica did not form on the membrane in short term DCMD process but

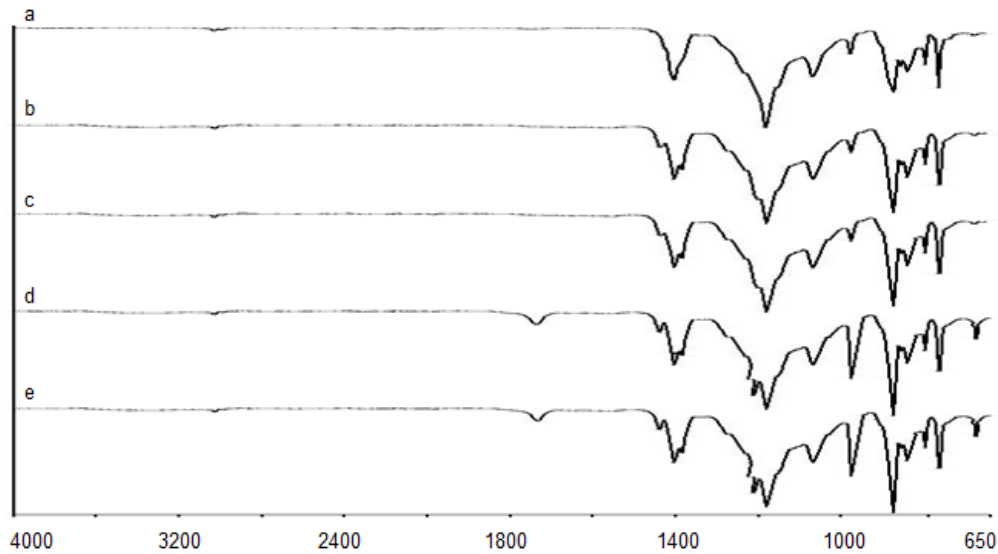


Fig. 8 FT-IR analysis (a) Clean membrane, (b)  $\Delta T = 20^\circ\text{C}$ ,  $v = 0.337$  m/s and  $t = 6$  hours, (c)  $\Delta T = 50^\circ\text{C}$ ,  $v = 0.337$  m/s and  $t = 6$  hours, (d)  $\Delta T = 50^\circ\text{C}$ ,  $v = 0.73$  m/s and  $t = 50$  hours, (e)  $\Delta T = 40^\circ\text{C}$ ,  $v = 0.73$  m/s and  $t = 75$  hours

silica was accumulated on the membrane in long term applications. No significant difference was observed between the spectra obtained from the fouled membranes in the DCMD system operated for a long period of time at  $\Delta T$  of  $40^\circ\text{C}$  and  $\Delta T$  of  $50^\circ\text{C}$ . The fact that the  $900\text{ cm}^{-1}$  peak in membrane measurement spectra of long term operations (Figs. 8d and 8e) belongs to Si-O is a verification of this. Music *et al.* (2011) carried out a study in which they reported that the peaks were observed at the  $370\text{-}1190\text{ cm}^{-1}$  in the  $\text{SiO}_2$  spectrum.

In MD, the salts such as  $\text{CaSO}_4$  are more soluble on the membrane surface in comparison with bulk feed solution due to decrease in their solubility with increasing temperature. Therefore, it is more difficult to crystallize on the membrane surface compared in bulk solution. The temperature of CTBD may be reduced for delaying membrane fouling. Moreover, considering the data in Fig. 5, while water recovery is about 60% up to the 38<sup>th</sup> hour corresponding to the start of flux decrease for  $\Delta T$  of  $50^\circ\text{C}$ , decrease in flux at  $\Delta T$  of  $40^\circ\text{C}$ , started on the 70<sup>th</sup> hour and the water recovery until this time was calculated as 70%. As a consequence, operating DCMD at  $\Delta T$  of  $40^\circ\text{C}$  is more advantageous due to reasons such as membrane fouling, delay of flux decrease, water recovery and operating cost even though the initial flux is low.

As for the distillate quality, the changes in operating conditions such as  $\Delta T$  and circulation rate did not play a role on the permeate quality for short term DCMD applications. The distillate properties obtained as a result of 6 hour applications were close to those of pure water. Likewise, the permeate characterization of the long term DCMD applications, prior to sudden flux decrease, resembled that of short term applications. However, distillate conductivity at  $\Delta T$  of  $50^\circ\text{C}$  was higher in comparison with that of  $\Delta T$  of  $40^\circ\text{C}$ . No distinctive change was observed in the analyses carried out after sudden flux decrease.

## 5. Conclusions

Power plants run out huge amounts of water for energy production and a certain amount of this water after use is discharged to the aquatic environment. Therefore, the recovery of the discharged wastewater is significant for the environment. Of separation and purification technologies, the MD process takes increasing attention, in recent years, in view of economic, operating and maintenance parameters. In this study, recovery of CTBD was studied by DCMD at different  $\Delta T$  and circulation rates. Permeate flux increased with increasing  $\Delta T$  and circulation rate in short term applications. While no distinctive fouling develops on the membrane during short term experiments, membrane fouling was observed in long term operating. The fouling on the membrane surface constituting of calcite ( $\text{CaCO}_3$ ), gypsum ( $\text{CaSO}_4 \cdot 2\text{H}_2\text{O}$ ) and silica causes a decrease in permeate flux. Permeate flux remained constant for 70 hours at  $\Delta T$  of  $40^\circ\text{C}$  during the long term DCMD application and the permeate flux decreased by 56% at the end of this period due to the fouling. Distillate conductivity slightly increased, reaching  $8\ \mu\text{S}/\text{cm}$  at the end of 70 hours. To retard the flux decline, application of pretreatments such as flocculation-sedimentation can be applied.

## Symbols

J:	Flux ( $\text{L}/\text{m}^2 \cdot \text{h}$ )
W:	Distillate water weight (kg)
A:	Membrane area ( $\text{m}^2$ )
t:	Time (hour)
R:	Rejection efficiency (%)
Re:	Reynolds number (unitless)
$\rho$ :	Density ( $\text{kg}/\text{m}^3$ )
$\vartheta$ :	Velocity (m/s)
D:	Hydraulic diameter (m)
$\mu$ :	Viscosity of the fluid ( $\text{kg}/\text{m} \cdot \text{s}$ )

## Abbreviations

ΔT	Transmembrane Temperature Difference
AGMD	Air Gap Membrane Distillation
C	Carbon
Ca	Calcium
CTBD	Cooling Tower Blowdown Water
DCMD	Direct Contact Membrane Distillation
DCOD	Dissolved Chemical Oxygen Demand
EDS	Energy Distribution Spectrometer
F	Fluor
FT	Feed Temperature
FTIR	Fourier Transformation Infrared
MD	Membrane Distillation
MF	Microfiltration
Mg	Magnesium
NF	Nanofiltration
NPOC	Non-Purgeable Organic Carbon
O	Oxygen
PP	Polypropylene
PT	Permeate Temperature
PTFE	Polytetrafluoroethylene
PVDF	Poly Vinylidene Fluoride
RO	Reverse osmosis
S	Sulphur
SEM	Scanning Electron Microscopy
SGMD	Sweeping Gas Membrane Distillation
Si	Silicium
TCOD	Total Chemical Oxygen Demand
TDS	Total Dissolved Solids
TKN	Total Kjeldahl Nitrogen
TOC	Total Organic Carbon
TSS	Total Suspended Solids
UF	Ultrafiltration
VMD	Vacuum Membrane Distillation

## References

- A.P.H.A. (2005), *Standard Methods for the Examination of Water and Wastewater*, (21<sup>st</sup> Edition), American Public Health Association, Washington, DC., USA.
- Borden, J., Gilron, J. and Hasson, D. (1987), "Analysis of RO flux decline due to membrane surface blockage", *Desalination*, **66**, 257-269. [https://doi.org/10.1016/0011-9164\(87\)90209-8](https://doi.org/10.1016/0011-9164(87)90209-8).
- Boubakri, A., Hafiane, A. and Bouguecha, S.A.T. (2017), "Direct contact membrane distillation: Capability to desalt raw water", *Arab. J. Chem.*, **10**, S3475-S3481. <https://doi.org/10.1016/j.arabjc.2014.02.010>.
- Dehghan, N., Nezakati, R. and Marandi, R. (2010), "Performance Evaluation of Yazd Combined Cycle Power Plant wastewater treatment system and the reuse of wastewater in agriculture", *The Second National Seminar on the Status of Recycled Waters in Water Resources Management*, Mashhad, Iran.
- Di Filippo, M.N. (2004), *Use of Produced Water in Recirculating Cooling Systems at Power Generating Facilities*, National Energy Technology Laboratory, Palo Alto, CA, USA.
- El-Bourawi, M.S., Ding, Z., Ma, R. and Khayet, M. (2006), "Review - A framework for better understanding membrane distillation separation process", *J. Membr. Sci.*, **285**, 4-29. <https://doi.org/10.1016/j.memsci.2006.08.002>.
- Ge, J., Peng, Y., Li, Z., Chen, P. and Wang, P. (2014), "Membrane fouling and wetting in a DCMD process for RO brine concentration", *Desalination*, **344**, 97-107. <https://doi.org/10.1016/j.desal.2014.03.017>.
- Greenlee, L.F., Lawler, D.F., Freeman, B.D., Marrot, B. and Moulin, P. (2009), "Reverse osmosis desalination: Water sources, technology, and today's challenges", *Water Res.*, **43**, 2317-2348. <https://doi.org/10.1016/j.watres.2009.03.010>.
- Gryta, M. (2009), "Calcium sulphate scaling in membrane distillation process", *Chem. Pap.*, **63** (2), 146-151. <https://doi.org/10.2478/s11696-008-0095-y>.
- Gryta, M. (2010), "Application of membrane distillation process for tap water purification", *Membr. Water Treat.*, **1**(1), 1-12. <https://doi.org/10.12989/mwt.2010.1.1.001>.
- Gryta, M. (2012), "Effectiveness of water desalination by membrane distillation process", *Membranes*, **2**, 415-429. <https://doi.org/10.3390/membranes2030415>.
- He, K., Hwang, H.J., Woo, M.W. and Moon, I.S. (2011), "Production of drinking water from saline water by direct contact membrane distillation (DCMD)", *J. Ind. Eng. Chem.*, **17**, 41-48. <https://doi.org/10.1016/j.jiec.2010.10.007>.
- Hou, D., Wang, J., Zhao, C., Wang, B., Luan, Z. and Sun, X. (2010), "Fluoride removal from brackish groundwater by direct contact membrane distillation", *J. Environ. Sci.*, **22**(12), 1860-1867. [https://doi.org/10.1016/S1001-0742\(09\)60332-6](https://doi.org/10.1016/S1001-0742(09)60332-6).
- Ji, X., Curcio, E., Al-Obaidani, S., Di Profio, G., Fontanova, E. and Drioli, E. (2010), "Membrane distillation-crystallization of seawater reverse osmosis brines", *Sep. Purif. Technol.*, **71**, 76-82. <https://doi.org/10.1016/j.seppur.2009.11.004>.
- Kim, S., Park, K.Y. and Cho, J. (2017), "Evaluation of the efficiency of cleaning method in direct contact membrane distillation of digested livestock wastewater", *Membr. Water Treat.*, **8**(2), 113-123. <https://doi.org/10.12989/mwt.2017.8.2.113>.
- Koyuncu, I. and Wiesner, M.R. (2007), "Morphological variations of precipitated salts on NF and RO membranes", *Environ. Eng. Sci.*, **24**, 602-614. <https://doi.org/10.1089/ees.2006.0114>.
- Kujawa, J. and Kujawski, W. (2015), "Driving force and activation energy in air-gap membrane distillation process", *Chem. Pap.*, **69**(11), 1438-1444. <https://doi.org/10.1515/chempap-2015-0155>.
- Liu, Q., Song, L., Zhang, Z. and Liu, X. (2010), "Preparation and characterization of the PVDF-based composite membrane for direct methanol fuel cells", *Int. J. Energy Environ.*, **1**(4), 643-656.
- Loussif, N. and Orfi, J. (2016), "Comparative study of air gap, direct contact and sweeping gas membrane distillation configurations", *Membr. Water Treat.*, **7**(1), 71-86. <https://doi.org/10.12989/mwt.2016.7.1.071>.
- Manna, A.K., Sen, M., Martin, A.R. and Pal, P. (2010), "Removal of arsenic from contaminated groundwater by solar driven membrane distillation", *Environ. Poll.*, **158**, 805-811. <https://doi.org/10.1016/j.envpol.2009.10.002>.
- Martinez-Diez, L. and Vazquez-Gonzalez, M.I. (1999), "Temperature and concentration polarization in membrane distillation of aqueous salt solutions", *J. Membrane Sci.*, **156**, 265-273. [https://doi.org/10.1016/S0376-7388\(98\)00349-4](https://doi.org/10.1016/S0376-7388(98)00349-4).
- Mattson, J.V. and Harris, T.G.I. (1979), "Zero discharge of cooling water by side stream softening", *J. Water Pollut. Control Fed.*, **51**, 2602-2614.
- Meng, S.W., Yea, Y., Mansouri, J. and Chen, V. (2015), "Crystallization behavior of salts during membrane distillation with hydrophobic and superhydrophobic capillary membranes", *J. Membr. Sci.*, **473**, 165-176. <https://doi.org/10.1016/j.memsci.2014.09.024>.
- Mohsen, M.S. (2004), "Treatment and reuse of industrial effluents: case study of a thermal power plant", *Desalination*, **167**, 75-86. <https://doi.org/10.1016/j.desal.2004.06.115>.
- Musić, S., Filipović-Vinceković, N. and Sekovanić, L. (2011), "Precipitation of amorphous SiO<sub>2</sub> particles and their properties", *Braz. J. Chem. Eng.*, **28**(1), 89-94. <http://dx.doi.org/10.1590/S0104-66322011000100011>.

- Pal, P. and Manna, A.K. (2010), "Removal of arsenic from contaminated groundwater by solar-driven membrane distillation using three different commercial membranes", *Wat. Res.*, **44**, 5750-5760. <https://doi.org/10.1016/j.watres.2010.05.031>.
- Peng, P., Fane, A.G. and Li, X. (2005), "Desalination by membrane distillation adopting a hydrophilic membrane", *Desalination*, **173**, 45-54. <https://doi.org/10.1016/j.desal.2004.06.208>.
- Plakas, K.V. and Karabelas, A.J. (2012), "Removal of pesticides from water by NF and RO membranes - A review", *Desalination*, **287**, 255-265. <https://doi.org/10.1016/j.desal.2011.08.003>.
- Saffarini, R.B., Mansoor, B., Thomas, R. and Arafat, H.A. (2013), "Effect of temperature-dependent microstructure evolution on pore wetting in PTFE membranes under membrane distillation conditions", *J. Membr. Sci.* **429**, 282-294. <https://doi.org/10.1016/j.memsci.2012.11.049>.
- Shintani, T., Matsuyama, H. and Kurata, N. (2009) "Effect of heat treatment on performance of chlorine-resistant polyamide reverse osmosis membranes", *Desalination*, **247**, 370-377. <https://doi.org/10.1016/j.desal.2008.09.003>.
- Shirazi, M.M.A., Kargari, A. and Shirazi, M.J.A. (2012), "Direct contact membrane distillation for seawater desalination", *Desalin. Water Treat.*, **49**, 368-375. <https://doi.org/10.1080/19443994.2012.719466>.
- Shirazi, M.M.A. and Kargari, A. (2015), "A Review on applications of membrane distillation (MD) process for wastewater treatment". *J. Membr. Sci. Res.*, **1**, 101-112. <https://dx.doi.org/10.22079/jmsr.2015.14472>.
- Wang, Z., Fan, Z.F., Xie, L.X. and Wang, S.C. (2006), "Study of integrated membrane systems for the treatment of wastewater from cooling towers", *Desalination*, **191**, 117-124. <https://doi.org/10.1016/j.desal.2005.04.125>.
- Yu, X., Yanga, H., Lei, H. and Shapiro, A. (2013), "Experimental evaluation on concentrating cooling tower blowdown water by direct contact membrane distillation", *Desalination*, **323**, 134-141. <https://doi.org/10.1016/j.desal.2013.01.029>.
- Zhang, J.D., Chen, L., Zeng, H.M., Yan, X.X., Song, X.N., Yang, H. and Ye, C.S. (2007), "Pilot testing of outside-in MF and UF modules used for cooling tower blowdown pretreatment of power plants", *Desalination*, **214**, 287-298. <https://doi.org/10.1016/j.desal.2006.12.004>.
- Zougrana, A., Çakmakci, M., Zengin, İ.H., İnoğlu, Ö. and Elcik, H. (2016), "Treatment of metal-plating waste water by modified direct contact membrane distillation", *Chem. Pap.*, **70**(9), 1185-1195. <https://doi.org/10.1515/chempap-2016-0066>.